Cooperative Peak Shaving and Voltage Regulation in Unbalanced Distribution Feeders

Yifei Guo, *Member, IEEE*, Qianzhi Zhang, *Student Member, IEEE*, and Zhaoyu Wang, *Senior Member, IEEE*

***Abstract*—This paper considers the co-operation of distributed generators (DGs), battery energy storage systems (BESSs) and voltage regulating devices for integrated peak shaving and voltage regulation in distribution grids through a co-optimization framework, which aims to minimize the operational costs while fulfilling the operational constraints of network and devices. To account for the uncertainties of load demand and generation, we then convert the co-optimization model into a two-stage stochastic program where state-of-charge (SoC) trajectories of BESSs and operation of voltage regulating devices are optimized at the first stage for day-ahead scheduling, while the reactive powers of DGs and BESSs are left at the second stage for potential intra-day scheduling to handle short-term voltage issues. The proposed co-optimization scheme is validated on the IEEE 37-node test feeder and compared with other practices.**

***Index Terms*—Battery energy storage system (BESS), co-optimization, distributed generator (DG), peak shaving, two-stage stochastic programming, voltage regulation.**

NOMENCLATURE

A. Sets

$N := \{0, 1, \ldots, n\}$	Set of buses
N_i^+	Set of children buses of bus i
$E \subseteq N \times N$	Set of branches
$T := \{1, \ldots, 24\}$	Set of time intervals
Φ_i, Φ_{ij}	Phase sets of bus i and branch (i, j)
Ξ	Set of scenarios

B. Parameters

ΔT	Time resolution [h]
V_n	Nominal bus voltage
λ_{ele}	Predicted electricity price [$/kWh]
λ_{bat}	Battery degradation cost [$/kWh]
λ_{cell}	Battery cell price [$/kWh]
λ_{tap}	Adjustment cost of on-load tap changer [$/time]
λ_{cap}	Switching cost of capacitor bank [$/time]
$V^{\min}, V^{\max}$	Min./max. voltage magnitude limits
$I_{ij}^{\max}$	Max. current limit of branch (i, j)
ΔTap_{ij}	Tap ratio change per step
$\Delta q_{i,\varphi}^c$	Capacity per bank at bus i, phase φ
$\Delta K_{ij,\varphi}^{\max}$	Tap change limit per time step
$\Delta K_{ij,\varphi}^{\mathrm{tot}}$	Total tap change limit over T
$K_{ij,\varphi}^{\min}, K_{ij,\varphi}^{\max}$	Min./max. tap position at branch (i, j)
$B_{i,\varphi}^{\max}$	Number of capacitor banks at bus i, phase φ
$\Delta B_{i,\varphi}^{\mathrm{tot}}$	Allowable changes of capacitor banks at bus i, phase φ
$Peak$	Peak load limit
$\overline{S}^{\mathrm{tr}}$	Transformer capacity
$\overline{S}_{i,\varphi}^g$	DG capacity at bus at bus i, phase φ
$\overline{p}_{i,\varphi,t}^g$	Available power of DG
$SoC^{\min}, SoC^{\max}$	Min./max. operation limits of SoC
$\overline{S}_{i,\varphi}^b$	BESS power rating at bus i, phase φ
$\overline{E}_{i,\varphi}$	BESS energy rating at bus i, phase φ
$\eta^{\mathrm{ch}}, \eta^{\mathrm{dc}}$	BESS charging/discharging efficiency
$\overline{Ir}$	Max. solar irradiance level
$z_{ij} \in \mathbb{C}^{\lvert\Phi_{ij}\rvert\times\lvert\Phi_{ij}\rvert}$	Impedance matrix of branch (i, j)

C. Variables

$s_{i,\varphi}^b$	Complex power injection from BESS at bus i, phase φ; $s_i^b := [s_{i,\varphi}^b]_{\varphi\in\Phi_i}$
$s_{i,\varphi}^c$	Complex power injection from capacitor banks at bus i, phase φ; $s_i^c := [s_{i,\varphi}^c]_{\varphi\in\Phi_i}$
$s_{i,\varphi}^g$	Complex DG power injection at bus i, phase φ; $s_i^g := [s_{i,\varphi}^g]_{\varphi\in\Phi_i}$
$s_{i,\varphi}^d$	Complex load consumption at bus i, phase φ; $s_i^d := [s_{i,\varphi}^d]_{\varphi\in\Phi_i}$
$v_i \in \mathbb{H}^{\lvert\Phi_i\rvert\times\lvert\Phi_i\rvert}$	Complex voltage matrix at bus i
$I_{ij} \in \mathbb{C}^{\lvert\Phi_{ij}\rvert\times 1}$	Complex line current from buses i to j
$K_{ij,\varphi}$	Tap position at branch (i, j)
$B_{i,\varphi}$	Number of capacitor banks connected at bus i
$K_{ij,\varphi}^+, K_{ij,\varphi}^-$	Auxiliary variables regarding tap changer on branch (i, j), phase φ
$B_{i,\varphi}^+, B_{i,\varphi}^-$	Auxiliary variables regarding capacitor banks at bus i, phase φ
$b_{i,\varphi}^{\mathrm{dc}}, b_{i,\varphi}^{\mathrm{ch}}$	Charging/discharging power of BESS at bus i, phase φ
$\mu_{i,\varphi,t}$	Indicator of charging/discharging status of BESS at bus i, phase φ
$S_{ij} \in \mathbb{C}^{\lvert\Phi_{ij}\rvert\times\lvert\Phi_{ij}\rvert}$	Complex power flow from buses i to j

Manuscript received August 10, 2020; revised December 26, 2020 and March 20, 2021; accepted March 27, 2021. This work was supported in part by the U.S. Department of Energy Wind Energy Technologies Office under Grant DE-EE0008956 and in part by the National Science Foundation under ECCS
Q1 1929975. *(Corresponding author: Zhaoyu Wang.)*

The authors are with the Department of Electrical and Computer Engineering, Iowa State University, Ames, IA 50011 USA (e-mail: yifeig@iastate.edu; qianzhi@iastate.edu; wzy@iastate.edu).

Color versions of one or more figures in this article are available at https://doi.org/10.1109/TPWRS.2021.3069781.

Digital Object Identifier 10.1109/TPWRS.2021.3069781

$l_{ij} \in \mathbb{C}^{\lvert\Phi_{ij}\rvert \times \lvert\Phi_{ij}\rvert}$	Squared current matrix
$\Lambda_{ij,t} \in \mathbb{C}^{\lvert\Phi_{ij}\rvert \times 1}$	Approximate diagonal entries of S_{ij}
$SoC_{i,\varphi}$	SoC of battery at bus i, phase φ
C	Overall operational cost
C_{ele}	Electricity purchase cost
C_{bat}	Operational cost of BESS degradation
C_{tap}	Operational cost of tap changers
C_{cap}	Operational cost of capacitor banks
Ir	Solar irradiance level

D. Operators

$(\cdot)^*$	Element-wise conjugate operator
$(\cdot)^T$	Transpose operator
$(\cdot)^H$	Complex-conjugate transpose operator
$\mathrm{Re}\{\cdot\}, \mathrm{Im}\{\cdot\}$	Real and imaginary parts of a complex number
$\mathrm{Tr}(\cdot)$	Trace of a matrix
$\mathbb{E}_{\xi}\{\cdot\}$	Expectation operator
$(\cdot)_t$	Variable at time t

I. Introduction

A. Background and Motivation

In recent decades, a variety of government policy-based incentives have supported the growth of distributed generators (DGs) such as wind, photovoltaic (PV), fuel cells, biomass, etc. Indeed, DGs bring technical, economic and environmental benefits; however, they may in turn incur new operational stress, e.g., power quality and network congestion issues [1]. Battery energy storage system (BESS) is arguably the most promising solution to aid the integration of renewables since it can be deployed in a modular and distributed fashion [2], [3]. Clearly, with a high penetration of renewable-based DGs, the real load profile may significantly deviate from the forecast, which will affect the utility companies' bidding behaviors in the wholesale electricity market. Correspondingly, the feeder voltage profile will vary with the net load. Hence, in a nutshell, while the ongoing deployment of renewables and BESSs poses challenges to energy management of distribution systems, it facilitates the revolution to exploit renewables in a cost-effective way at the same time.

Peak shaving and voltage/reactive power (volt/var) regulation are the two fundamental functionalities in distribution management systems. Peak shaving is a process of flattening the load profile by shifting peak load demand to off-peak periods via energy storage and/or demand side management [7]. It benefits the entire power systems including power plants, system operators as well as end-users. Particularly, for system operators, effective peak shaving can postpone the expensive upgrades for transmission and distribution systems. The primary goal of volt/var regulation is, as the name suggests, maintaining the feeder voltages within a feasible range (e.g., 0.95–1.05 p.u. in ANSI Standard C84.1 [8]) by scheduling the voltage regulating devices, e.g., on-load tap changers (OLTCs), step-voltage regulators (SVRs) and capacitor banks [9]. Moreover, the advanced four-quadrant inverter-interfaced DGs and BESSs are capable of providing fast and continuous volt/var support locally [4], [5], which can alleviate the work loads on the legacy devices [6].

Thanks to the conventional *separate* operation of peak shaving and volt/var regulation [9], a substantial body of studies have solely investigated either peak shaving or volt/var regulation for a long time; see [7] and [10], [11] for surveys on these two isolate topics, respectively. However, the practical operation reveals the fact that they interact with each other due to the physical nature of power network: i) reshaping the load profile also reshapes the voltage profile, especially for some low-voltage feeders with high R/X ratios; and ii) regulating voltages can lower the peak load via reducing line losses and load demand [12].

In light of this, the co-operation of peak shaving and voltage regulation becomes appealing since it can maximize the usage of DGs and storage, thereby unlocking additional benefits in terms of operational cost, power quality, supply reliability as well as network reinforcement, which cannot be well accomplished by the traditional separate architectures.

B. Literature Review

A few studies have addressed the co-operation between peak shaving and volt/var regulation, especially for the planning of DGs and BESSs considering the operation conditions. Several rule-based control algorithms have been proposed in [13]–[15]. However, they rely on the heuristic design without providing system-wide optimality guarantees.

Several studies have bridged the methodology gap by developing optimization frameworks. In [16], the authors investigate the potential of BESSs in deferring upgrades needed to host a higher penetration of PV, where an optimal power flow (OPF) problem is formulated with the aim of mitigating voltage deviation and reducing peak load restricted by limited capital and operation and maintenance costs of BESSs. In [17], an optimization model that minimizes BESS cost, voltage deviation, voltage unbalance and peak demand charge together, is built. It should be noted that the weight allocation on multiple heterogeneous objectives as in [16], [17] is usually tricky. A short-term scheduling scheme of BESSs is proposed in [18] to address peak shaving, volt/var regulation and reliability enhancement simultaneously, by solving an OPF program using Tabu search. In [19], a bi-level scheduling strategy is developed, consisting of the bidding in day-ahead market (DAM) to minimize the overall costs in supplying the net load and a real-time dispatch to compensate for the energy gap. However, [16]–[19] mainly focus on the operation of BESSs, neglecting the coordination with voltage regulating devices.

To address such issue, [20]–[22] further have the legacy voltage regulating devices participate in the co-operation. In [20], a two-stage optimal dispatch framework is proposed for distribution grids with distributed wind, where the peak shaving and volt/var regulation are implemented in a *successive* coordinated fashion instead of the so-called *co-optimization* in a strict sense. The authors in [21] develop an integrated framework for conservation voltage reduction and demand response to reduce the energy bills of customers. In [22], a model predictive control scheme is proposed to minimize network losses or energy purchase cost whilst maintaining voltages within limits by co-optimizing the operation of OLTCs, PV inverters and BESSs in two different timescales (1 h and 15-min). Besides, [20]–[22] address the prediction uncertainties of DGs and load by leveraging the scenario-based stochastic programming techniques with one-stage [20], [21] or two-stage models [22]. However, only balanced feeders are considered.

C. Contributions

In spirit, this work is close to [19]–[21] which consider a day-ahead multi-step scheduling of DGs and BESSs to enhance utilities' bidding strategies in the DAM. However, we contribute in the following distinct ways:

1) Firstly, we, for the first time, propose a comprehensive co-optimization framework for an integrated peak shaving and volt/var regulation by scheduling DGs, BESSs and voltage regulating devices. This framework aims to minimize the overall operational costs including energy purchase, battery degradation, as well as wear and tear of tap changers and capacitor banks, while satisfying the operational constraints. The unbalanced case is especially addressed by generalizing the linear multi-phase branch flow model to incorporate tap changers, rendering the problem computationally tractable.
2) Secondly, to account for the forecast uncertainties of renewables and load while relieving the conservative behavior of a robust decision, we propose to reformulate the problem into a two-stage stochastic program. It is noteworthy that, with this two-stage model, only the SoC trajectories of BESSs and voltage regulating devices will be actually implemented in day-ahead operation whereas the reactive powers of DGs and BESSs are left for a re-scheduling.
3) Lastly, we demonstrate the proposed co-optimization unlocks additional revenue in comparison to the successive optimization method and also demonstrate that only relying on cost reduction does *not* necessarily lower the peak load. This implies that an explicit peak load limit should be imposed in the co-optimization.

The rest of this paper is organized as follows. Section II presents the deterministic formulation of the co-optimization problem. In Section III, the optimization problem is reformulated as a two-stage stochastic program accounting for uncertainties. Section IV presents the numerical results, followed by conclusions.

II. Problem Formulation

This section presents the problem formulation of the co-optimization framework for day-ahead cooperative peak shaving and volt/var regulation over the time horizon of 24 h with 1-h time resolution compatible with the DAM. Fig. 1 presents the overview of the proposed framework.

A. Objective Function

The co-optimization framework aims to minimize the overall operational costs including energy purchase, battery degradation, as well as wear-and-tear of tap changers and capacitor banks during T, which is mathematically given as follows:

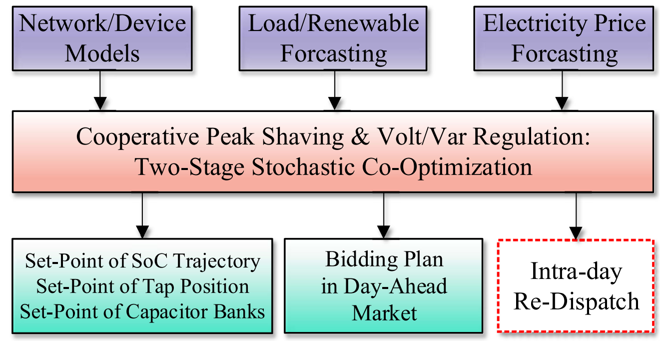

Fig. 1. Schematic diagram of the proposed day-ahead co-optimization framework for cooperative peak shaving and volt/var regulation. Though the intra-day dispatch is not explicitly addressed in this work, the proposed two-stage stochastic programming methodology remains its potential in the second stage.

1) Electricity Purchase Cost:

$$C_{\mathrm{ele}} := \sum_{t\in T} \lambda_{\mathrm{ele},t} \Bigg(\mathrm{Re}\left\{\mathrm{Tr}(S_{01,t})\right\} + \sum_{(i,j)\in E} \mathrm{Re}\{\mathrm{Tr}(z_{ij} l_{ij,t})\} \Bigg) \Delta T \quad (1)$$

where the first part is the feed-in power flow from the substation (that does not include the line losses) and the second term represents the total line losses.

2) Battery Degradation Cost:

$$C_{\mathrm{bat}} := \sum_{t\in T}\sum_{i\in N}\sum_{\varphi\in\Phi_i} \lambda_{\mathrm{bat}} \left|\mathrm{Re}\left\{s^b_{i,\varphi,t}\right\}\right| \Delta T. \quad (2)$$

3) Operational Cost of Tap Changer:

$$C_{\mathrm{tap}} := \sum_{t\in T}\sum_{(i,j)\in E}\sum_{\varphi\in\Phi_{ij}} \lambda_{\mathrm{tap}} \left|K_{ij,\varphi,t} - K_{ij,\varphi,t-1}\right|. \quad (3)$$

4) Operational Cost of Capacitor Bank:

$$C_{\mathrm{cap}} := \sum_{t\in T}\sum_{i\in N}\sum_{\varphi\in\Phi_i} \lambda_{\mathrm{cap}} \left|B_{i,\varphi,t} - B_{i,\varphi,t-1}\right|. \quad (4)$$

Accordingly, the overall cost function is given by,

$$C := C_{\mathrm{ele}} + C_{\mathrm{bat}} + C_{\mathrm{tap}} + C_{\mathrm{cap}}. \quad (5)$$

B. Constraints

1) Multi-Phase Power Flow: The convex relaxation techniques, e.g., second-order cone programming (SOCP) relaxation [24], [25] and semidefinite programming (SDP) relaxation [26], [27], are usually leveraged to convexify the nonlinear power flow equations. Some applications can be observed in the existing works related to our topic. For example, the works [21] and [22] use the SOCP relaxation to convexify the OPF programs but it cannot be easily extended to unbalanced cases due to the mutual impedance of feeders [28]. The SDP relaxation is applicable to unbalanced systems; however, it may be computationally expensive, especially in the presence of discrete variables. Moreover, the exactness of relaxation may not be guaranteed. Thus, to make the optimization problem computationally tractable, we generalize the linear multi-phase branch flow model [27] to incorporate a tap changer, which is as, for any branch $(i, j) \in E$,

$$\Lambda_{ij,t} = s^d_{j,t} - s^g_{j,t} - s^b_{j,t} - s^c_{j,t} + \sum_{k \in N_j^+} \Lambda^{\Phi_j}_{jk,t}, t \in T \quad (6)$$

$$S_{ij,t} = (aa^H)^{\Phi_{ij}} \mathrm{diag}\left(\Lambda_{ij,t}\right), t \in T \quad (7)$$

$$v^{\Phi_{ij}}_{i,t} = v_{j,t} - k_{ij,t} v_0^{\Phi_{ij}} + S_{ij,t} z^H_{ij} + z_{ij} S^H_{ij,t}, t \in T \quad (8)$$

where $a := [1, e^{-\mathbf{i}2\pi/3}, e^{\mathbf{i}2\pi/3}]^T$; $k_{ij,t} := [k_{ij,\varphi\varphi',t}]_{\varphi,\varphi' \in \Phi_{ij}}$ with the entries being,

$$k_{ij,\varphi\varphi',t} = \left(K_{ij,\varphi,t} + K_{ij,\varphi',t}\right) \Delta Tap_{ij},\ \varphi, \varphi' \in \Phi_{ij}. \quad (9)$$

It is understood that $k_{ij,t} = \mathrm{diag}(1, 1, 1)$ always holds for each branch without a tap changer.

Besides, to estimate the line losses, the line current can be approximately captured as, for any $(i, j) \in E$,

$$\Lambda_{ij,t} = V_n \mathrm{diag}(a^{\Phi_{ij}} I^H_{ij,t}),\ t \in T \quad (10)$$

$$l_{ij,t} = I_{ij,t} I^H_{ij,t},\ t \in T. \quad (11)$$

The linear approximation represented by (6)–(11) is based on the assumption that the network is not too severely unbalanced and operates around the nominal voltage. This is widely believed to hold in practice if it is with effective voltage regulation.

2) Network Operation Security: The operational limits of bus voltage and line current are as follows:

$$(V^{\min})^2 \le \mathrm{diag}(v_{i,t}) \le (V^{\max})^2,\ i \in N, t \in T \quad (12)$$

$$\mathrm{diag}(l_{ij,t}) \le (I^{\max}_{ij})^2,\ (i, j) \in E, t \in T. \quad (13)$$

3) Peak Load Demand: Additionally, we consider a hard constraint of net peak load during a day,

$$\mathrm{Re}\left\{\mathrm{Tr}(S_{01,t})\right\} + \sum_{(i,j) \in E} \mathrm{Re}\{\mathrm{Tr}(z_{ij} l_{ij,t})\} \le Peak,\ t \in T. \quad (14)$$

Imposing an explicit constraint is of great significance for effective peak shaving because only relying on cost reduction does not necessarily lower the peak load. This will be demonstrated later. Keep in mind that a very low peak limit could render the problem infeasible due to the limited BESS capacity. In this paper, an easy-to-implement way is leveraged to determine the peak limit value—we gradually lower the peak limit until the problem becomes infeasible. In this way, the maximum peak shaving potential can be known.

4) Substation Transformer: The transformer capacity limit is expressed as,

$$\left\| \begin{bmatrix} \mathrm{Re}\{\mathrm{Tr}(\mathrm{S}_{01,t})\} \\ \mathrm{Im}\{\mathrm{Tr}(S_{01,t})\} \end{bmatrix} \right\|_2 \le \overline{S}^{\mathrm{tr}}, t \in T \quad (15)$$

where to reduce the computation complexity, line losses are neglected here since this constraint generally is not truly binding considering the feed from DGs and a slight overloading of transformer is allowed for a short period.

5) Tap Changer: The operational constraints of tap changer over branch are given by, for any $(i, j) \in E$ and $\varphi \in \Phi_{ij}$,

$$K^{\min}_{ij,\varphi} \le K_{ij,\varphi,t} \le K^{\max}_{ij,\varphi},\ K_{ij,\varphi,t} \in \mathbb{Z}, t \in T \quad (16)$$

$$|K_{ij,\varphi,t} - K_{ij,\varphi,t-1}| \le \Delta K^{\max}_{ij,\varphi},\ t \in T \quad (17)$$

$$\sum_{t \in T} |K_{ij,\varphi,t} - K_{ij,\varphi,t-1}| \le \Delta K^{\mathrm{tot}}_{ij,\varphi} \quad (18)$$

where (16) denotes the tap position limits; (17) constrains the tap change during a sampling time interval; and (18) constrains the total operation times of tap changers during T.

6) Capacitor Bank: The operational constraints of capacitor banks are given as, for any bus $i \in N$ and $\varphi \in \Phi_i$,

$$\mathrm{Re}\{s^c_{i,\varphi,t}\} = 0, t \in T \quad (19)$$

$$\mathrm{Im}\{s^c_{i,\varphi,t}\} = B_{i,\varphi,t} \Delta q^c_{i,\varphi},\ t \in T \quad (20)$$

$$0 \le B_{i,\varphi,t} \le B^{\max}_{i,\varphi},\ B_{i,\varphi,t} \in \mathbb{Z},\ t \in T \quad (21)$$

$$\sum_{t \in T} |B_{i,\varphi,t} - B_{i,\varphi,t-1}| \le \Delta B^{\mathrm{tot}}_{i,\varphi} \quad (22)$$

where (20) denotes the total reactive power injected by capacitor banks; (21) constrains the maximum number of capacitor banks; (22) constrains the maximum switching times of capacitor banks during T.

7) Battery Energy Storage: In this paper, we consider the lithium-ion battery—one of the most popular options today. If we limit the battery operation within certain depth of discharge region to avoid the overcharge and over-discharge, there is a constant marginal cost for the cycle depth increase. In this way, the battery degradation cost can be prorated with respect to charged and discharged energy into a per-kWh cost [29],

$$\lambda_{\mathrm{bat}} = \frac{\lambda_{\mathrm{cell}}}{2M(SoC^{\max} - SoC^{\min})} \quad (23)$$

where M is the number of cycles that the battery could be operated within $[SoC^{\min}, SoC^{\max}]$.

The model and operational constraints of a BESS at $\varphi \in \Phi_i$ of bus $i \in N$ can be expressed as,

$$\mathrm{Re}\{s^b_{i,\varphi,t}\} = b^{\mathrm{dc}}_{i,\varphi,t} - b^{\mathrm{ch}}_{i,\varphi,t},\ t \in T \quad (24)$$

$$0 \le b^{\mathrm{ch}}_{i,\varphi,t} \le \mu_{i,\varphi,t} \cdot \overline{S}^b_{i,\varphi},\ t \in T \quad (25)$$

$$0 \le b^{\mathrm{dc}}_{i,\varphi,t} \le (1 - \mu_{i,\varphi,t}) \cdot \overline{S}^b_{i,\varphi},\ t \in T \quad (26)$$

$$\mu_{i,\varphi,t} \in \{0, 1\},\ t \in T \quad (27)$$

$$SoC_{i,\varphi,t} = SoC_{i,\varphi,t-1} + \left(b^{\mathrm{ch}}_{i,\varphi,t} \eta^{\mathrm{ch}} - \frac{b^{\mathrm{dc}}_{i,\varphi,t}}{\eta^{\mathrm{dc}}}\right) \frac{\Delta T}{\overline{E}_{i,\varphi}}, t \in T \quad (28)$$

$$SoC^{\min} \le SoC_{i,\varphi,t} \le SoC^{\max},\ t \in T \quad (29)$$

$$SoC_{i,\varphi,0} = SoC_{i,\varphi,24} \quad (30)$$

$$\left\| \begin{bmatrix} \mathrm{Re}\{\mathrm{s}^{\mathrm{b}}_{\mathrm{i},\varphi,\mathrm{t}}\} \\ \mathrm{Im}\{s^b_{i,\varphi,t}\} \end{bmatrix} \right\|_2 \le \overline{S}^b_{i,\varphi},\ t \in T. \quad (31)$$

Constraints (24)–(27) represent the real power model of a BESS. Constraint (28) represents the physical model of SoC of a BESS while (29)–(30) represent its operational constraints. As shown in (30), the SoC levels at the beginning and the end of a day should be equal so that the framework can periodically operate. (31) constrains the apparent power of BESS converter that restricts the real and reactive power in a coupling way.

8) Inverter-Based DG: A four-quadrant inverter-interfaced DG at $\varphi \in \Phi_i$ of bus $i \in N$ is modeled by,

$$\mathrm{Re}\left\{s^{g}_{i,\varphi,t}\right\} = \overline{p}^{g}_{i,\varphi,t}, t \in T \tag{32}$$

$$\left\| \begin{bmatrix} \mathrm{Re}\{s^{g}_{i,\varphi,t}\} \\ \mathrm{Im}\{s^{g}_{i,\varphi,t}\} \end{bmatrix} \right\|_2 \leq \overline{S}^{g}_{i,\varphi},\ t \in T \tag{33}$$

where it is assumed that the PV system operates with the maximum power tracking mode (track $\overline{p}^{g}_{i,\varphi,t}$). [1]

Clearly, for each bus i that does not have capacitor banks, BESS or DG installation, we have $s^{c}_{i,t} = 0, s^{g}_{i,t} = 0$ or $s^{b}_{i,t} = 0$, respectively.

C. Reformulation and Compact Expression

The objectives (2)–(4) and constraints (18) and (22) contain the sum of absolute terms with respect to the tap position and capacitor banks, which are not tractable for off-the-shelf solvers. Thus, we reformulate them by introducing the auxiliary variables $K^{+}_{ij,\varphi}, K^{-}_{ij,\varphi}$ $B^{+}_{i,\varphi}$ and $B^{-}_{i,\varphi}$ [similar reformulation has been given in (24)–(27) for BESSs]. Then, constraint (18) can be equivalently rewritten as,

$$K_{ij,\varphi,t} - K_{ij,\varphi,t-1} = K^{+}_{ij,\varphi,t} - K^{-}_{ij,\varphi,t}, t \in T \tag{34}$$

$$\sum_{t\in T}\left(K^{+}_{ij,\varphi,t} + K^{-}_{ij,\varphi,t}\right) \leq \Delta K^{\mathrm{tot}}_{ij,\varphi} \tag{35}$$

$$K^{+}_{ij,\varphi,t} \geq 0, K^{-}_{ij,\varphi,t} \geq 0, K^{+}_{ij,\varphi,t}, K^{-}_{ij,\varphi,t} \in \mathbb{Z}, t \in T. \tag{36}$$

Similarly, constraint (22) becomes,

$$B_{i,\varphi,t} - B_{i,\varphi,t-1} = B^{+}_{i,\varphi,t} - B^{-}_{i,\varphi,t}, t \in T \tag{37}$$

$$\sum_{t\in T}\left(B^{+}_{i,\varphi,t} + B^{-}_{i,\varphi,t}\right) \leq \Delta B^{\mathrm{tot}}_{i,\varphi} \tag{38}$$

$$B^{+}_{i,\varphi,t} \geq 0, B^{-}_{i,\varphi,t} \geq 0, B^{+}_{i,\varphi,t}, B^{-}_{i,\varphi,t} \in \mathbb{Z}, t \in T. \tag{39}$$

Correspondingly, the cost functions $C_{\mathrm{tap}}, C_{\mathrm{cap}}$ as well as C_{bat} can be rewritten as,

$$C_{\mathrm{tap}} = \sum_{t\in T}\sum_{(i,j)\in E}\sum_{\varphi\in\Phi_{ij}} \lambda_{\mathrm{tap}}\left(K^{+}_{ij,\varphi,t} + K^{-}_{ij,\varphi,t}\right) \tag{40}$$

$$C_{\mathrm{cap}} = \sum_{t\in T}\sum_{i\in N}\sum_{\varphi\in\Phi_{i}} \lambda_{\mathrm{cap}}\left(B^{+}_{i,\varphi,t} + B^{-}_{i,\varphi,t}\right) \tag{41}$$

$$C_{\mathrm{bat}} = \sum_{t\in T}\sum_{i\in N}\sum_{\varphi\in\Phi_{i}} \lambda_{\mathrm{bat}}\left(b^{\mathrm{ch}}_{i,\varphi,t} + b^{\mathrm{dc}}_{i,\varphi,t}\right)\Delta T. \tag{42}$$

Finally, the optimization problem is abstractly expressed as,

$$\text{(DP): } \underset{u\in\mathcal{U}}{\text{minimize}}\ \ C(u) \tag{43a}$$

$$\text{subject to }\ g(u) \leq 0 : \begin{cases} (12)–(17),(21) \\ (25)–(27),(29),(31) \\ (33),(35),(36),(38),(39) \end{cases} \tag{43b}$$

$$h(u) = 0 : \begin{cases} (1),(5),(6)–(11),(19) \\ (20),(24),(28),(30),(32) \\ (34),(37),(40)–(42) \end{cases} \tag{43c}$$

where u is the compact decision vector of all the decisions; $\mathcal{U}$ is the Cartesian product of real, complex and integer number sets, which characterizes u in an element-wise manner.

So far, the deterministic problem formulation (DP) has been given in (43), which is inherently a mixed-integer second-order cone program (MISOCP) that can be handled by off-the-shelf solvers, e.g., CPLEX, MOSEK, etc.

III. Stochastic Programming Formulation

The day-ahead operation scheduling establishes on the load, renewable generation and electricity price, etc. However, due to various uncertainties, e.g. stochastic nature of the load and renewables, it is difficult to forecast them with very high accuracy. Therefore, we consider the forecast uncertainties of load and renewables by converting the deterministic optimization program DP into a two-stage stochastic program, while allowing for re-dispatching reactive power resources.

A. Scenario Generation and Reduction

The load consumption prediction error is calculated based on a truncated normal distribution [30]. The solar power generation is dependent on the incident solar irradiance, while the irradiance significantly depends on the cloud coverage condition. Therefore, the solar irradiance prediction error is modeled by introducing a correction factor to the prediction $\overline{Ir}$ with a clear weather, following a normal distribution that depends on the given cloud coverage level [31],

$$Ir = \overline{Ir}(1-\varepsilon),\ \varepsilon = [\mathrm{Norm}(\mu_\varepsilon, \sigma_\varepsilon)]_0^1 \tag{44}$$

where $[\cdot]_0^1$ denotes the projection onto the set [0,1].

Based on the known probability distributions, Monte-Carlo simulation is conducted to create a required number of scenarios for solar irradiance and load. They are then reduced to a given number of scenarios by the backward reduction method, of which more details can be referred to [32].

B. Two-Stage Stochastic Programming Formulation

Firstly, we split $u \in \mathcal{U}$ into two groups, i.e., $u := \{x, y\}$ and $\mathcal{U} := \mathcal{X} \times \mathcal{Y}$ where

- x represents the decision variables associated with the charging/discharging of BESSs, operation of tap changers and operation of capacitor banks themselves.
- y consists of all the remaining variables.

Correspondingly, the cost function and constraints in DP can be reconstructed as,

$$C(u) \Rightarrow C_1(x) + C_2(y) \tag{45}$$

$$h(u) \Rightarrow h_1(x) = 0\ \cap\ h_2(x,y) = 0 \tag{46}$$

[1] To allow for real power curtailment, one can replace "=" by "≤" in (32).

$$g(u) \Rightarrow g_1(x) \le 0 \ \cap \ g_2(x,y) \le 0 \tag{47}$$
$$u \in \mathcal{U} \Rightarrow x \in \mathcal{X} \cap y \in \mathcal{Y} \tag{48}$$

where $C_1(x)$ corresponds to $C_{\text{bat}} + C_{\text{tap}} + C_{\text{cap}}$ while $C_2(y)$ corresponds to C_{ele}.

Then, define a realization of stochastic scenario as $\xi := \{p^g_{i,\varphi,t}, s^d_{i,\varphi,t}\}_{i\in N, t\in T}$, a two-stage stochastic counterpart of DP can be formulated as,

$$\text{(SP): } \underset{x\in\mathcal{X}}{\text{minimize}} \ C_1(x) + \mathbb{E}_\xi \left\{ \underset{y\in\mathcal{Y}}{\text{minimize}} \ C_2(y;\xi) \right\} \tag{49a}$$
$$\text{subject to} \ \ h_1(x) = 0 \tag{49b}$$
$$g_1(x) \le 0 \tag{49c}$$
$$h_2(x,y;\xi) = 0 \tag{49d}$$
$$g_2(x,y;\xi) = 0 \tag{49e}$$

where x corresponds to the first-stage (here-and-now) decisions before the realization of ξ and y corresponds to the second-stage (wait-and-see) corrective actions under a given realization of ξ. The independent control variables at the first stage include the charging/discharging power of BESSs $\text{Re}\{s^b_{i,\varphi,t}\}$, the operation trajectories of tap changers $K_{ij,t}$ and the operation trajectories of capacitor banks $s^c_{i,t}$. The second-stage control variables are the reactive powers of BESSs and DGs, i.e., $\text{Im}\{s^b_{i,\varphi,t}\}$ and $\text{Im}\{s^g_{i,\varphi,t}\}$.

C. Deterministic Equivalent

Representing the uncertainties through a finite scenario set $\Xi := \{\xi_1, \ldots, \xi_{|\Xi|}\}$ with the probability distribution $\rho_1, \ldots, \rho_{|\Xi|}$, the approximate deterministic equivalent problem of SP in the extensive form can be given as,

$$\text{(SP-d): } \underset{x\in\mathcal{X}, y_k\in\mathcal{Y}}{\text{minimize}} \ C_1(x) + \sum_{k=1}^{|\Xi|} \rho_k C_2(y_k;\xi_k) \tag{50a}$$
$$\text{subject to} \ \ h_1(x) = 0 \tag{50b}$$
$$g_1(x) \le 0 \tag{50c}$$
$$h_2(x,y_k;\xi_k) = 0, \ k = 1, \ldots, |\Xi| \tag{50d}$$
$$g_2(x,y_k;\xi_k) = 0, \ k = 1, \ldots, |\Xi| \tag{50e}$$

which is inherently an extensive MISOCP program that can be also directly handled by conic programming solvers.

D. Robustness

In practice, the prior probability distributions regarding load and solar may be inaccurate. Interestingly, the proposed two-stage stochastic co-optimization framework is robust against it in the sense that the reactive power capabilities of DGs are considered in the day-ahead co-optimization, but the reactive powers of DGs are not directly dispatched in a day-ahead manner. Instead, DGs will be re-dispatched according to the intra-day operational status of distribution networks (with more accurate load and PV data). In this way, the undesired operational status (e.g., voltage violations) induced by the inaccurate modeling of uncertainties can be corrected/compensated.

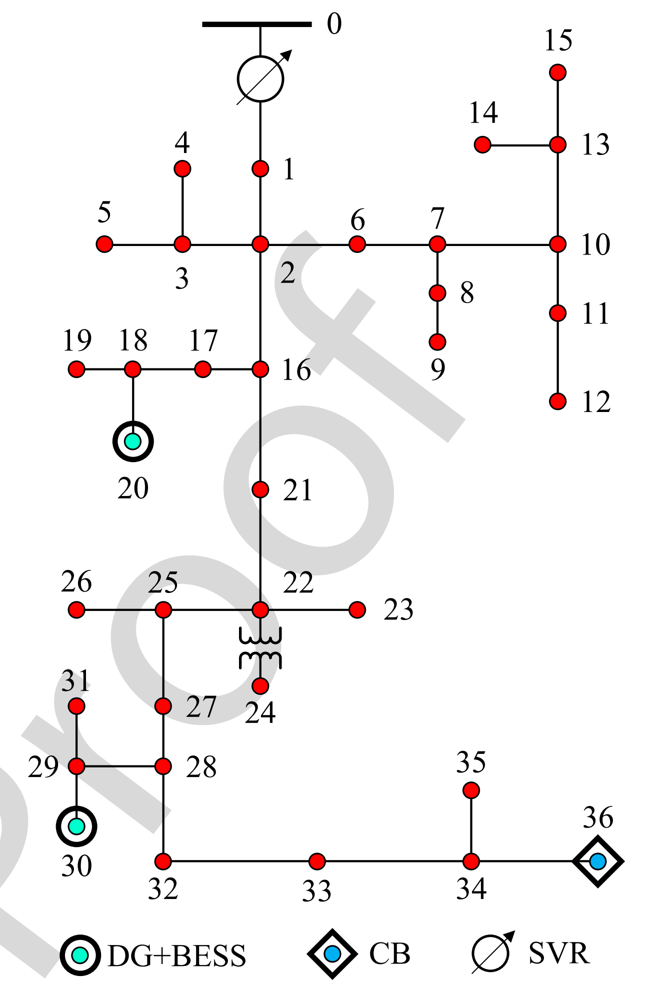

Fig. 2. Single-line diagram of IEEE 37-node test feeder. The original feeder is modified to include two phase-wise PV panels at Buses 20 and 30 with the rated capacities of 200 kVA and 300 kVA per phase. Two phase-wise BESSs with 500 kW/1500 kWh and 300 kVA/900 kWh power/energy ratings per phase at Buses 20 and 30, respectively. Besides, a capacitor bank with a rated capacity of 50 kVAr/unit and 100 kVAr in total per phase is installed at Bus 36.

IV. Numerical Results

The proposed co-optimization methodologies are tested on the modified IEEE 37-node test feeder (see Fig. 2) [33]. The SVR has an operation range of [0.9,1.1] p.u. with ±16 tap positions (i.e., $K^{\min} = -16, K^{\max} = 16$ and $\Delta Tap = 0.2/32$). The Lithium Manganese Oxide battery is considered for the simulation with a cell price of 0.5\$/Wh and $M = 10\,000$ cycles when the depth of discharge is 60% [29]. The SoC limits are set as $SoC^{\min} = 0.2$ and $SoC^{\max} = 0.8$. The per-unit costs associated with operation of the tap changer and capacitor banks are set as 1.40 \$/time and 0.24 \$/time, which can be adjusted as per the switching risk assessment of utilities [34]. The daily load profile of a real distribution feeder in Iowa, U.S. and a solar generation time series generated by a testbed [35] are used as

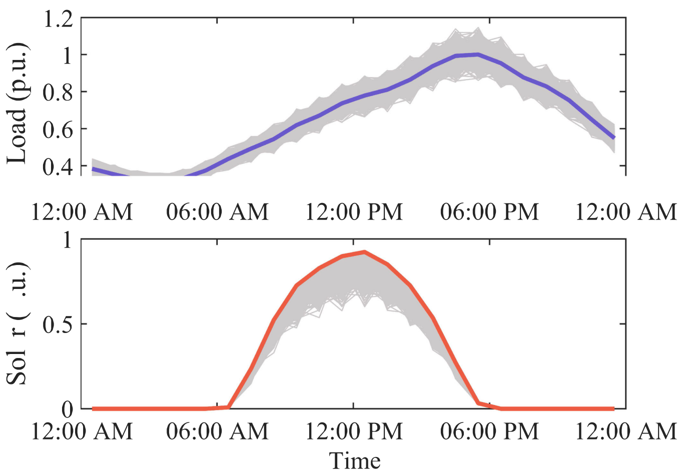

Fig. 3. Load and solar generation profiles (1-h resolution). The thick lines represent the predicted profiles while others are generated stochastic scenarios.

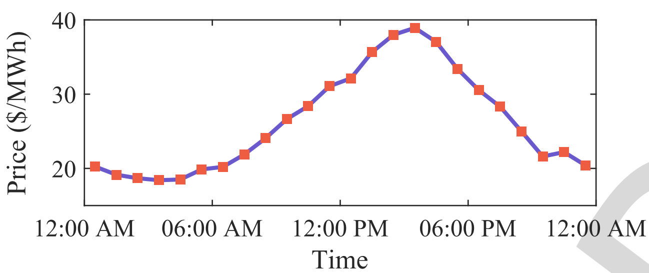

Fig. 4. Day-ahead locational marginal price in central Iowa at July 3 rd 2017 obtained from historical MISO market dataset.

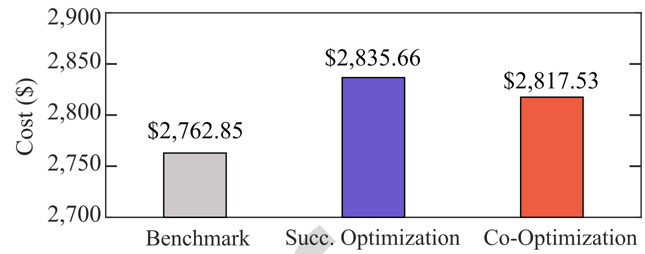

Fig. 5. Operational cost with different operation strategies.

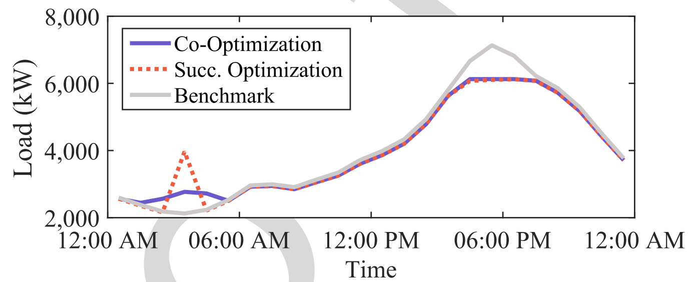

Fig. 6. Peak load performance with different operation strategies. To conduct a fair comparison (same peak load), the successive optimization strategy with a peak limit (without line losses) of 5700 MW is first tested and then the resultant actual peak load after voltage regulation (6100 MW, including line losses) is set as the peak limit in the co-optimization.

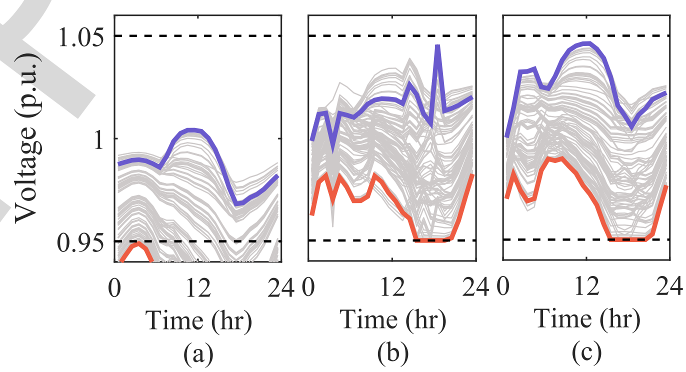

Fig. 7. Voltage performance with different operation strategies. (a) Benchmark; (b) successive optimization; (c) co-optimization. Each line represents a phase-wise voltage magnitude of a bus. The thick lines highlight the lowest and highest bus voltages within a day.

the predictions of load and maximum available solar generation (see Fig. 3). The locational marginal price obtained from historical MISO market dataset [36] is used as the forecasted electricity price in DAM (Fig. 4). For uncertainty modeling, as discussed before, it is assumed that the random load prediction error follows the truncated normal distribution where the mean value is the forecasted load, the standard deviation is 5% and the truncation bound is set as $\pm 15\%$, respectively; the solar irradiance correction factor follows the normal distribution with mean value $\mu_\varepsilon = 10\%$ and standard deviation $\sigma_\varepsilon = 5\%$. These parameters can be tuned per the given real data.

A. Co-Optimization v.s. Successive Optimization

In this section, we perform a comparison between the proposed co-optimization (cooperative peak shaving and volt/var regulation) and the successive coordinated optimization proposed in [20] to demonstrate the unlocked additional benefits by the proposed co-operation. For the successive optimization, the peak shaving and the volt/var optimization are performed in a successive way; for the benchmark, the distribution system operates without peak shaving and volt/var regulation. For the sake of clarity, this comparison is performed on a deterministic case. To better illustrate the effectiveness of the proposed method, the benchmark load demand in [33] is scaled up by four. As shown in Fig. 5, the operational costs with different optimization strategies are compared. It shows that the co-optimization strategy reduces the operational cost compared to the successive optimization one with the same peak load and voltage limits. As seen from Fig. 6, to achieve peak shaving, the load during peak times will be shifted to 12:00 AM–06:00 AM with relatively low prices by scheduling the BESSs. Utilities will thus purchase more electricity for this period. Besides, as shown in Figs. 7 (b) and (c), the voltage profiles with the two optimization methods are effectively regulated within the limits [0.95,1.05] p.u. But by comparison, the co-optimization results in smoother voltage variations. The benchmark has the lower operational costs because it does not include any operational costs of BESSs and

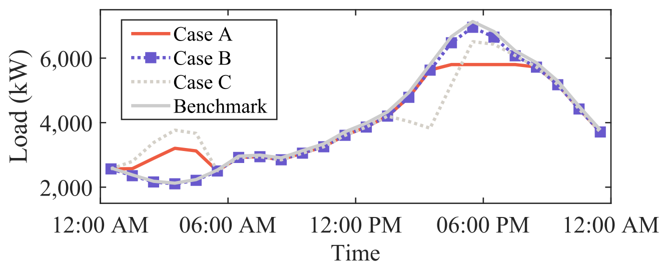

Fig. 8. Peak load performance with different operation strategies where in Case A, the co-optimization strategy is carried out with a peak load limit of 5800 MW; in Case B, the peak load limit is relaxed; and in Case C, the peak load limit and the operational costs of BESSs are both relaxed.

voltage regulating devices but most bus voltages significantly violate the lower limit while the peak load stays high.

B. Merit of an Explicit Peak Load Constraint

In this subsection, we examine the necessity of a hard and explicit peak load limit constraint in the co-optimization. As shown in Fig. 8, only relying on the cost reduction (Case B) does not effectively lower the peak load because the imposed operational cost of BESSs is more expensive than cost savings by leveraging the ToU price, though it does reduce the overall operational costs of the system. Without considering BESS costs in the optimization, it is observed that the peak load can be slightly reduced. But, consider that if we have sufficient available load shifting capability, there will be a trend that all the load will be shifted/aggregated to the periods with the lowest price. Therefore, there will be a new (and higher) peak at 04:00 AM. This demonstrates the necessity of an explicit constraint on peak load in the optimization problem.

C. Deterministic Optimization v.s. Stochastic Optimization

The comparison between the deterministic co-optimization and (single-stage and two-stage) stochastic co-optimization methods is carried out to demonstrate the value of stochastic programming. 1000 random scenarios of load and solar power time-series are generated as shown in Fig. 3 and are then reduced to 15 representative scenarios, which strives for a balance between performance and computational complexity. 100 new random scenarios are generated to test the performance of different methods under uncertainties. The deterministic co-optimization solves (43). The single-stage stochastic co-optimization solves x and y in one stage (same solution for all scenarios) based on the reduced scenario set. The two-stage stochastic co-optimization solves (50) based on the reduced scenario set, which only yields x; and then in the tests, it allows solving y again with fixed x to simulate the intra-day re-dispatch under a given test scenario. Fig. 9 compares the voltage performance among different optimization methods. We record the highest and lowest value voltage magnitude of all buses after 100 random Monte-Carlo simulations. It can be observed that some voltage buses (especially for Phase C) with the DP violate the lower limit under some scenarios since it does not consider the uncertainties from load and solar in the optimization. The single-stage stochastic

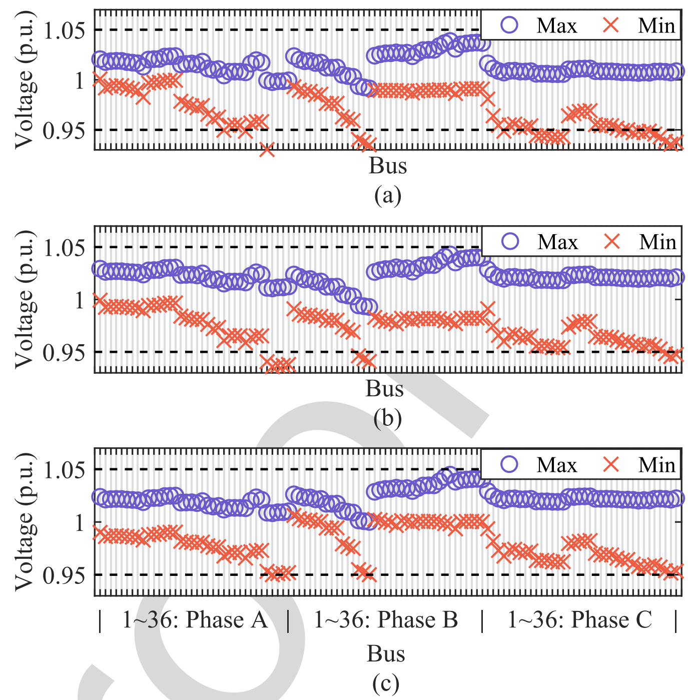

Fig. 9. Voltage performance (min./max. magnitude) with (a) deterministic optimization, (b) singe-stage stochastic optimization and (c) two-stage stochastic optimization where the maximum and minimum values of all (phase-wise) bus voltages during a day among the 100 test scenarios are presented.

optimization strategy schedules all the controllable devices in one stage together considering the uncertain prediction errors and thus, it alleviates the voltage violations in Phase C but there are still several bus voltages lower than 0.95 p.u. In comparison, the two-stage stochastic optimization framework regulates all the bus voltages within the ANSI limit since it considers the uncertainties and allows a re-scheduling of reactive powers of BESSs and solar inverters, thereby exhibiting better robustness. This justifies the necessity of the intra-day re-scheduling of available controllable devices. Fig. 10 gives the comparison in terms of peak shaving performance. It can be observed that, with the deterministic optimization, the peak load violates 6000 kW in most of scenarios with the highest peak of 6856.4 kW; the single-stage stochastic optimization alleviates the violation with the highest peak of 6450.1 kW. By contrast, the two-stage optimization can effectively regulate the peak load (maximum peak load 6087.5 kW). The rationale behind this can be elaborated as follows. Obviously, since the deterministic optimization does not take into account any uncertainties in the decision making, it has no robustness against it. The stochastic optimization also violates the peak limit because the reduced scenario space cannot cover all the possible scenarios but it performs better than the deterministic optimization. The single-stage stochastic optimization model considers the uncertainties but does not allow different reactive power outputs from DGs and BESSs under different scenarios. In comparison, given the two-stage model allows for re-dispatching reactive power outputs of DGs and BESSs at the second stage (so-called "wait-and-see"), the network losses can be further reduced under different scenarios

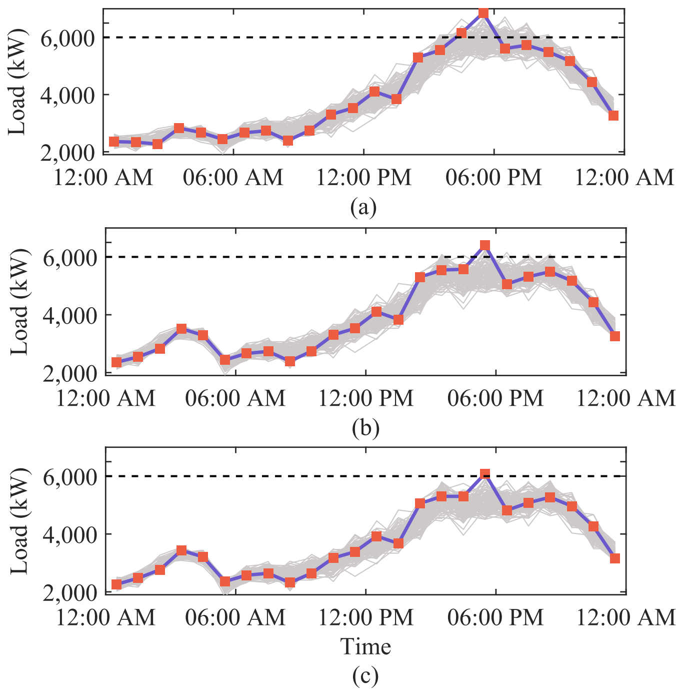

Fig. 10. Peak load performance with deterministic, one-stage stochastic and two-stage stochastic optimization. (a) deterministic; (b) one-stage stochastic optimization; (c) two-stage stochastic optimization. Each line represents the real power load of distribution system under a given stochastic scenario. The thick line represents the scenario with the highest peak load.

so that a lower peak load can be achieved. This validates the merit of stochastic optimization and the necessity of re-dispatch.

V. Conclusion

This paper addresses the day-ahead cooperative operation of peak shaving and voltage regulation in an unbalanced distribution through a joint optimization framework. We then consider the uncertainties of load and solar by converting the co-optimization model into a two-stage stochastic program. The numerical results show that the proposed co-optimization framework brings more cost benefits than the successive optimization method while effectively regulating the voltages and peak load within the limits. Furthermore, due to the consideration of uncertainties and the enabled re-dispatch, the proposed two-stage stochastic programming method facilitates robust operations. Besides, we also verify the necessity of an explicit peak load constraint in the optimization for effective peak shaving.

For large-scale networks with a number of stochastic scenarios, the efficiency of centralized solution may be challenged. Therefore, the distributed solution framework is required for better scalability. We leave it for future work.

References

[1] S. Kakran and S. Chanana, "Smart operations of smart grids integrated with distributed generation: A review," *Renewable Sustain. Energy Rev.*, vol. 81, pp. 524–535, Jan. 2018.

[2] B. Dunn, H. Kamath, and J.-M. Tarascon, "Electrical energy storage for the grid: A battery of choices," *Science*, vol. 334, no. 6058, pp. 928–935, 2011.

[3] S. Comello and S. Reichelstein, "The emergence of cost effective battery storage, *Nat. Commun.*, vol. 10 no. 1, pp. 1–9, 2019.

[4] Y. Guo, Q. Wu, H. Gao, X. Chen, J. Østergaard, and H. Xin, "MPC-based coordinated voltage regulation for distribution networks with distributed generation and energy storage system," *IEEE Trans. Sustain. Energy*, vol. 10. no. 4, pp. 1731–1739, Oct. 2019.

[5] A. Colmenar-Santos, C. Reino-Rio, D. Borge-Diez, and E. Collado Fernandez, "Distributed generation: A review of factors that can contribute most to achieve a scenario of DG units embedded in the new distribution networks," *Renewable Sustain. Energy Rev.*, vol. 59, pp. 1130–1148, 2016.

[6] Y. Guo, Q. Wu, H. Gao, S. Huang, B. Zhou and C. Li, "Double-timescale coordinated voltage control in active distribution networks based on MPC," *IEEE Trans. Sustain. Energy*, vol. 11, no. 1, pp. 294–303, Jan. 2020.

[7] M. Uddin, M. F. Romlie, M. F. Abdullah, S. A. Halim, A. H. A. Bakar, and T. C. Kwang, "A review on peak load shaving strategies," *Renewable Sustain. Energy Rev.*, vol. 82, pp. 3323–3332, Feb. 2018.

[8] *American National Standard for Electric Power Systems and Equipment.Voltage Ratings (60 Hz)*, ANSI C84.1.2011 Standard. Q2

[9] R. Singh *et al.*, "Foundational report series: Advanced distribution management systems for grid modernization, DMS industry survey," Argonne Nat. Lab., Lemont, IL, USA, Tech. Rep., Apr. 2017.

[10] H. Sun *et al.*, "Review of challenges and research opportunities for voltage control in smart grids," *IEEE Trans. Power Syst.*, vol. 34, no. 4, pp. 2790–2801, Jul. 2019.

[11] K. E. Antoniadou-Plytaria, I. N. Kouveliotis-Lysikatos, P. S. Georgilakis, and N. D. Hatziargyriou, "Distributed and decentralized voltage control of smart distribution networks: Models, methods, and future research," *IEEE Trans. Smart Grid*, vol. 8, no. 6, pp. 2999–3008, Nov. 2017.

[12] J. Carden and D. Popovic, "Closed-loop volt/var optimization: Addressing peak load reduction," *IEEE Power Energy Mag.*, vol. 16, no. 2, pp. 67–75, Mar. 2018

[13] J. Zupančič, E. Lakić, T. Medved, and A. Gubina, "Advanced peak shaving control strategies for battery storage operation in low voltage distribution network," in *Proc. IEEE Manchester PowerTech*, Jun. 2017. Q3

[14] M. J. E. Alam, K. M. Muttaqi, and D. Sutanto, "Mitigation of rooftop solar PV impacts and evening peak support by managing available capacity of distributed energy storage systems," *IEEE Trans. Power Syst.*, vol. 28, no. 4, pp. 3874–3884, Nov. 2013.

[15] Y. Yang, H. Li, A. Aichhorn, J. Zheng, and M. Greenleaf, "Sizing strategy of distributed battery storage system with high penetration of photovoltaic for voltage regulation and peak load shaving," *IEEE Trans. Smart Grid*, vol. 5, no. 2, pp. 982–991, Mar. 2014.

[16] J. Tant, F. Geth, D. Six, P. Tant, and J. Driesen, "Multiobjective battery storage to improve PV integration in residential distribution grids," *IEEE Trans. Sustain. Energy*, vol. 4, no. 1, pp. 182–191, Jan. 2013.

[17] N. Jayasekara, M. A. S. Masoum, and P. J. Wolfs, "Optimal operation of distributed energy storage systems to improve distribution network load and generation hosting capability," *IEEE Trans. Sustain. Energy*, vol. 7, no. 1, pp. 250–261, Jul. 2016.

[18] M. Sedghi, A. Ahmadian, and M. Aliakbar-Golkar, "Optimal storage planning in active distribution network considering uncertainty of wind power distributed generation," *IEEE Trans. Power Syst.*, vol. 31, no. 1, pp. 304–316, Jan. 2016.

[19] Y. Zheng *et al.*, "Optimal operation of battery energy storage system considering distribution system uncertainty," *IEEE Trans. Sustain. Energy*, vol. 9, no. 3, pp. 1051–1060, Jul. 2018.

[20] B. Zhou, D. Xu, K. W. Chan, C. Li, Y. Cao, and S. Bu, "A two-stage framework for multiobjective energy management in distribution networks with a high penetration of wind energy," *Energy*, vol. 135, pp. 754–766, Jul. 2017.

[21] M. S. Hossan and B. Chowdhury, "Integrated CVR and demand response framework for advanced distribution management systems," *IEEE Trans. Sustain. Energy*, vol. 11, no. 1, pp. 534–544, Jan. 2020.

[22] R. Zafar, J. Ravishankar, J. E. Fletcher, and H. R. Pota, "Multi-timescale model predictive control of battery energy storage system using conic relaxation in smart distribution grids," *IEEE Trans. Power Syst.*, vol. 33, no. 6, pp. 7152–7161, Nov. 2018.

[23] Z. Taylor *et al.*, "Customer-side SCADA-assisted large battery operation optimization for distribution feeder peak load shaving," *IEEE Trans. Smart Grid*, vol. 10, no. 1, pp. 992–1004, Jan. 2019.

[24] R. A. Jabr, "Radial distribution load flow using conic programming," *IEEE Trans. Power Syst.*, vol. 21, no. 3, pp. 1458–1459, Aug. 2006.

[25] M. Farivar and S. H. Low, "Branch flow model: Relaxations and convexification—Part I," *IEEE Trans. Power Syst.*, vol. 28, no. 3, pp. 2554–2564, Aug. 2013.

[26] X. Bai, H. Wei, K. Fujisawa, and Y. Wang, “Semidefinite programming for optimal power flow problems,” *Int. J. Elect. Power Energy Syst.*, vol. 30, no. 6/7, pp. 383–392, 2008.

[27] L. Gan and S. H. Low, “Convex relaxations and linear approximation for optimal power flow in multiphase radial networks,” in *Proc. Power Syst. Comput. Conf.*, 2014, pp. 1–9.

[28] B. A. Robbins and A. D. Domínguez-García,, “Optimal reactive power dispatch for voltage regulation in unbalanced distribution systems,” *IEEE Trans. Power Syst.*, vol. 31, no. 4, pp. 2903–2913, Jul. 2016.

[29] Y. Shi, B. Xu, D. Wang, and B. Zhang, “Using battery storage for peak shaving and frequency regulation: Joint optimization for superlinear gains,” *IEEE Trans. Power Syst.*, vol. 33. no. 3, pp. 2882–2894, May 2018.

[30] N. Lu, R. Diao, R. P. Hafen, N. Samaan, and Y. Makarov, “A comparison of forecast error generators for modeling wind and load uncertainty,” in *Proc. IEEE PES Gen. Meeting*, Vancouver, BC, Canada, 2013, pp. 1–5,.

[31] R. Torquato, Q. Shi, W. Xu, and W. Freitas, “A Monte Carlo simulation platform for studying low voltage residential networks,” *IEEE Trans. Smart Grid*, vol. 5, no. 6, pp. 2766–2776, Jul. 2014.

[32] J. Dupačová, N. Gröwe-Kuska, and W. Römisch, “Scenario reduction in stochastic programming: An approach using probability metrics,” *Math. Program.*, vol. A. 95, pp. 493–511, 2003.

[33] *IEEE*, “37 node distribution test feeder,” Aug. 2017. [Online]. Available: https://ewh.ieee.org/soc/pes/dsacom/testfeeders/

[34] P. Li *et al.*, “A coordinated control method of voltage and reactive power for active distribution networks based on soft open point,” *IEEE Trans. Sustain. Energy*, vol. 8, no. 4, pp. 1430–1442, Oct. 2017.

[35] C. Holcomb, “Pecan Street Inc.: A test-bed for NILM,” in *Proc. Int. Workshop Non-Intrusive Load Monit.*, 2012. [Online]. Available: https://www.pecanstreet.org/

[36] “MISO Market Data: *Historical LMP*,” Accessed: Sep. 2017. [Online]. Available: https://www.misoenergy.org/markets-and-operations/real-time -market-data/market-reports/#nt=

Yifei Guo (Member, IEEE) received the B.E. and Ph.D. degrees in electrical engineering from Shandong University, Jinan, China, in 2014 and 2019, respectively. He is currently a Postdoctoral Research Associate with the Department of Electrical and Computer Engineering, Iowa State University, Ames, IA, USA. He was a Visiting Student with the Department of Electrical Engineering, Technical University of Denmark, Lyngby, Denmark, from 2017–2018.

His research interests include voltage/var control, renewable energy integration, wind farm control, distribution system optimization and control, and power system protection.

Qianzhi Zhang (Student Member, IEEE) received the M.S. degree in electrical engineering from Arizona State University, in 2015. He is currently working toward the Ph.D. degree with the Department of Electrical and Computer Engineering, Iowa State University, Ames, IA. He was a Research Engineer with Huadian Electric Power Research Institute, from 2015–2016. His research interests include the applications of machine learning and optimization techniques in power system operation and control.

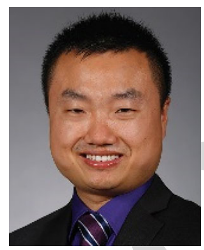

Zhaoyu Wang (Senior Member, IEEE)) received the B.S. and M.S. degrees in electrical engineering from Shanghai Jiaotong University, and the M.S. and Ph.D. degrees in electrical and computer engineering from the Georgia Institute of Technology. He is the Harpole-Pentair Assistant Professor with Iowa State University. His research interests include optimization and data analytics in power distribution systems and microgrids. He is the Principal Investigator for a multitude of projects focused on these topics and funded by the National Science Foundation, the Department of Energy, National Laboratories, PSERC, and Iowa Economic Development Authority. Dr. Wang is the Secretary of IEEE Power and Energy Society (PES) PSOPE Award Subcommittee, Co-Vice Chair of PES Distribution System Operation and Planning Subcommittee, and Vice Chair of PES Task Force on Advances in Natural Disaster Mitigation Methods. He is the Editor of IEEE TRANSACTIONS ON POWER SYSTEMS, IEEE TRANSACTIONS ON SMART GRID, IEEE OPEN ACCESS JOURNAL OF POWER AND ENERGY, IEEE POWER ENGINEERING LETTERS, and *IET Smart Grid*. He was the recipient of the National Science Foundation (NSF) CAREER Award, the IEEE PES Outstanding Young Engineer Award, and the Harpole-Pentair Young Faculty Award Endowment.